Effects of Temperature and $\Delta G°$ on Electron Transfer from Cytochrome c_2 to the Photosynthetic Reaction Center of the Purple Bacterium *Rhodobacter sphaeroides*

G. Venturoli,* F. Drepper,# J. C. Williams,§ J. P. Allen,§ X. Lin,§ and P. Mathis#

*Dipartimento di Biologia, Università di Bologna, Bologna I-40126, Italy; #DBCM, Section de Bioénergétique (CNRS, URA 2096), CEA Saclay, F-91191 Gif-sur-Yvette Cedex, France; §Department of Chemistry and Biochemistry and Center for the Study of Early Events in Photosynthesis, Arizona State University, Tempe, Arizona 85287-1604 USA

ABSTRACT The kinetics of electron transfer from cytochrome c_2 to the primary donor (P) of the reaction center from the photosynthetic purple bacterium *Rhodobacter sphaeroides* have been investigated by time-resolved absorption spectroscopy. Rereduction of P^+ induced by a laser pulse has been measured at temperatures from 300 K to 220 K in a series of specifically mutated reaction centers characterized by altered midpoint redox potentials of P^+/P varying from 410 mV to 765 mV (as compared to 505 mV for wild type). Rate constants for first-order electron donation within preformed reaction center–cytochrome c_2 complexes and for the bimolecular oxidation of free cytochrome c_2 have been obtained by multiexponential deconvolution of the kinetics. At all temperatures the rate of the fastest intracomplex electron transfer increases by more than two orders of magnitude as the driving force $-\Delta G°$ is varied over a range of 350 meV. The temperature and $\Delta G°$ dependences of the rate constant fit the Marcus equation well. Global analysis yields a reorganization energy $\lambda = 0.96 \pm 0.07$ eV and a set of electronic matrix elements, specific for each mutant, ranging from $1.2\ 10^{-4}$ eV to $2.5\ 10^{-4}$ eV. Analysis in terms of the Jortner equation indicates that the best fit is obtained in the classical limit and restricts the range of coupled vibrational modes to frequencies lower than $\sim$200 cm^{-1}. An additional slower kinetic component of P^+ reduction, attributed to electron transfer from cyt c_2 docked in a nonoptimal configuration of the complex, displays a Marcus type dependence of the rate constant upon $\Delta G°$, characterized by a similar value of λ (0.8 $\pm$ 0.1 eV) and by an average electronic matrix element smaller by more than one order of magnitude. In all of the mutants, as the temperature is decreased below 260 K, both intracomplex reactions are abruptly inhibited, their rate being negligible at 220 K. The free energy dependence of the second-order rate constant for oxidation of cyt c_2 in solution suggests that the collisional reaction is partially diffusion controlled, reaching the diffusion limit at exothermicities between 150 and 250 meV over the temperature range investigated.

INTRODUCTION

Electron transfer is a very simple reaction that is central to the function of proteins in many biological processes. This is well known in bioenergetics: photosynthesis and respiration realize energy conversion through a complex sequence of electron transfer reactions. However, electron transfer also takes place in many other biological processes, from cell defense to gene control. The rate of electron transfer from a donor D to an acceptor A is the key parameter that determines the biological function, and much effort has been exerted to relate the rate to structural and thermodynamic features.

When D and A are separated by more than $\sim$5 Å, electron transfer reactions can be treated in the nonadiabatic (weak coupling) limit. Electron transfer theory states that in such weakly coupled pairs, the rate constant k can be expressed by the Fermi golden rule:

$$k = \frac{2\pi}{\hbar} H_{DA}^2(\mathrm{FC}) \qquad (1)$$

where $\hbar$ is Planck's constant divided by 2π, H_{DA} is the electronic tunneling matrix element between donor and acceptor, and (FC) is the nuclear Franck-Condon factor that describes the nuclear motions associated with electron transfer (DeVault, 1984; Marcus and Sutin, 1985; Bertrand, 1991; Parson and Warshel, 1995).

The tunneling matrix element H_{DA} depends upon donor-acceptor separation and orientation and upon the nature of the intervening medium. In the simplest models, the electronic coupling H_{DA}^2 is predicted to drop exponentially with increasing donor-acceptor separation d (Hopfield, 1974; Jortner, 1976; DeVault, 1984; Marcus and Sutin, 1985):

$$H_{DA}^2(d) = H_{DA}^2(d_o)\exp[-\beta(d - d_o)] \qquad (2)$$

where $H_{DA}^2(d_o)$, the electronic coupling element at van der Waals contact distance d_o, includes the orientation dependence, and the coefficient β describes the overall effect of the intervening medium in propagating the wave function. From data spanning 20 Å in distance and 12 orders of magnitude in rate, Moser et al. (1992) found that Eq. 2 is compatible with many electron transfer reactions in biolog-

Received for publication 3 November 1997 and in final form 16 February 1998.

Address reprint requests to Dr. Giovanni Venturoli, Dipartimento di Biologia, Università di Bologna, via Imerio 42, Bologna I-40126, Italy. Tel.: 39-51-351-288; Fax: 39-51-242-576; E-mail: ventur@alma.unibo.it.

Dr. Drepper's present address is Institut für Biologie II/Biochemie, Universität Freiburg, Schänzlestrasse 1, D-79104 Freiburg, Germany.

Dr. Lin's present address is PerSeptive Biosystems, Framingham, MA 01701.

0006-3495/98/06/3226/15 $2.00

ical and semibiological systems when d is identified as the shortest distance between the centers of atoms at the edges of the donors and acceptors. This analysis, which considers the protein medium as a homogeneous glassy solvent, yields $\beta \approx 1.4$ Å^{-1}, a value intermediate between that estimated for electron transfer through vacuum ($\beta \approx 2.8$ Å^{-1}) and that between covalently bridged redox centers ($\beta \approx 0.7$ Å^{-1}). To explain more complex behaviors exhibited in proteins (Karpishin et al., 1994), models have been developed that take into account the inhomogeneity of the intervening protein medium (Kuki and Wolynes, 1987). The pathway-searching algorithm introduced by Beratan and Onuchic (Beratan et al., 1991) selects tunneling pathways between D and A by combining covalent, H-bonded, and through-space contacts in a way that maximizes the coupling. A given coupling pathway can be described in terms of an equivalent covalent pathway with an effective number of covalent bonds.

The Franck-Condon factor (FC) in Eq. 1 is commonly expressed in terms of the standard free energy of the reaction $\Delta G°$ and of the reorganization energy λ. The reorganization energy includes contributions from changes in bond lengths, bond angles, distances, and orientations involving the donor, the acceptor, and the medium. The Franck-Condon factor can be evaluated by using different approximations at various levels of sophistication (DeVault, 1984; Parson and Warshel, 1995). A classical treatment of nuclear motion in a harmonic approximation leads to the simplest and most widely used expression, derived by Marcus (Marcus and Sutin, 1985), which predicts a Gaussian dependence of the rate constant k on $\Delta G°$:

$$k = \frac{2\pi}{\hbar} H_{DA}^2 (4\pi\lambda k_B T)^{-(1/2)} \exp[-(\Delta G^o + \lambda)^2/(4\lambda k_B T)] \quad (3)$$

where k_B is the Boltzman constant and T is the temperature. The validity of Eq. 3 requires that electron transfer be coupled only to nuclear vibrations of low angular frequency ω, such that $\hbar\omega \ll k_B T$.

Based on quantum mechanical treatment of the thermally weighted Franck-Condon factors, general expressions have been derived that consider an arbitrary number of vibrational modes coupled to the electron transfer process (for reviews see DeVault, 1984; Parson and Warshel, 1995). More manageable expressions incorporating quantum effects have been developed for simplified cases, e.g., when the vibrational modes can be collected into one or two effective modes (Gunner and Dutton, 1989).

For a single vibrational mode of any angular frequency ω in a harmonic approximation, the following relation has been obtained (Jortner, 1976; DeVault, 1984):

$$k = \frac{2\pi}{\hbar^2\omega} H_{DA}^2 e^{-s(2n+1)} \left(\frac{n+1}{n}\right)^{(p/2)} I_p(2s[n(n+1)]^{1/2}) \quad (4)$$

where $s = \lambda/\hbar\omega$, $p = -\Delta G°/\hbar\omega$, $n = [\exp(\hbar\omega/k_B T) - 1]^{-1}$, and I_p refers to the modified Bessel function of order p. Equation 4 reduces to the classical Marcus equation (Eq. 3) in the high-temperature (or low-frequency) limit, when $\hbar\omega \ll k_B T$.

To check the validity of theoretical treatments, it is necessary to measure the rate of electron transfer under conditions in which several important parameters (such as T, $\Delta G°$, d, nature of the medium between D and A) are measurable and adjustable. Reaction centers (RCs) of photosynthetic organisms, especially purple bacteria, are particularly suitable because electron transfer is naturally triggered by light. They also have several advantages, such as well-known distances and redox properties; moreover, they can be manipulated by site-directed mutagenesis, and electron transfer rates can often be measured accurately in a broad range of temperatures (Boxer, 1990).

Several groups have studied electron transfer reactions within reaction centers of *Rhodobacter sphaeroides* and *Rhodopseudomonas viridis* in that perspective, measuring rates in mutants, at various temperatures, and attempting to provide a test for theoretical treatments. Three aspects are most difficult to evaluate: What is the value of the reorganization energy λ? What are the vibrational modes coupled to electron transfer? How should the microscopic properties of the medium separating D and A be taken into consideration? Other properties are often neglected, such as variations in $\Delta G°$ with temperature. Two reactions have been dealt with in some detail: electron transfer from bacteriopheophytin to the primary quinone acceptor Q_A (Gunner and Dutton, 1989), and back electron transfer from Q_A^- to the oxidized special pair P^+ (P is a bacteriochlorophyll dimer) (Feher et al., 1988; Gunner and Dutton, 1989; Ortega et al., 1996).

In this work we focus on the different case of electron transfer from a small protein, cytochrome (cyt) c_2, to an electron acceptor (P^+) located in the reaction center of *Rhodobacter* (*Rb.*) *sphaeroides*. The complete reaction involves diffusion of the partners, attraction of cyt c_2, binding, electron transfer, and dissociation. This situation is relevant to many cases of electron transfer between a small protein and another partner, such as between cytochrome *c* and cytochrome *c* oxidase (Pan et al., 1991; McLendon and Hake, 1992). The factors that control the rate of electron transfer involving soluble *c*-type cytochromes are far from being definitively elucidated. Estimates of the reorganization energy, based on kinetic studies performed in different systems, span a large range of values varying from 0.7 eV to 1.5 eV (McLendon and Hake, 1992), and, in some cases, could be affected by the energetics of bringing the reacting partners together to the effective distance for the electron transfer process. The determination of the reorganization energy in a well-characterized cytochrome *c* system thus is of particular interest.

There have been several studies on the interaction between cytochrome c_2 and the reaction center of *Rb. sphaeroides*. These studies have provided a kinetic model and elucidated the parameters controlling the docking and some aspects of the geometry of the complex (for a review see Tiede and Dutton, 1993; Adir et al., 1996; Drepper et al.,

1997; Drepper and Mathis, 1997). The multiphasic oxidation kinetics of the reaction of soluble *c*-type cytochromes with reaction centers have been extensively investigated (Overfield et al., 1979; Long et al., 1989; Tiede et al., 1993; Venturoli et al., 1993), leading to a well-established reaction scheme, which includes a first-order electron donation occurring within a preformed RC-cyt c_2 complex and a bimolecular process due to the reaction of cytochrome in solution. The observation of multiple first-order kinetic components has been attributed to intracomplex electron transfer from cyt c_2 docked in different configurations (Tiede et al., 1993; Lin et al., 1994b). Analogous kinetic heterogeneities in the electron transfer from the bound tetraheme cytochrome *c* to P^+ in *Rhodopseudomonas viridis* reaction centers have been suggested to reflect different substates of the complex (Ortega and Mathis, 1993).

Two parameters of electron transfer rate, temperature and $\Delta G°$, have been varied, systematically but separately, in previous experiments. Varying temperature, with wild-type reaction centers, revealed two properties (Venturoli et al., 1993). First it was shown that the reaction rate slows down slightly when temperature decreases from 295 K ($t_{1/2} = 410$ ns) to 244 K ($t_{1/2} = 2.3$ μs), reflecting an activation energy of 20.5 kJ · mol^{-1}. Second, it appeared that the extent of fast reduction of P^+ by cyt c_2 decreases steeply around 250 K, becoming negligible below 230 K. This property is still unexplained. It makes it impossible to measure the effect of temperature on the rate below ~240 K. The effect of $\Delta G°$ on the rate has also been studied, at 295 K, with a series of mutants in which the midpoint redox potential (*Em*) of the couple P^+/P is altered from +410 mV to +765 mV. The driving force $\Delta G°$ is varied accordingly, because $\Delta G° \approx Em(\text{cyt } c_2^{3+}/\text{cyt } c_2^{2+}) - Em(P^+/P)$. The values of the rate versus $-\Delta G°$ were fitted to a Marcus equation, with a reorganization energy $\lambda = 500$ meV and a maximum rate of 1.4×10^7 s^{-1} (Lin et al., 1994b).

We thought that it would be most useful to study the effect of temperature on the rate of electron transfer for the same series of mutants with different values of $\Delta G°$. This article reports the results of such a study, in which experimental data are subjected to a global analysis according to several models.

MATERIALS AND METHODS

Proteins

Reaction centers were isolated from semiaerobically grown cultures of *Rb. sphaeroides*, following a procedure described by Lin et al. (1994b). Purified concentrated reaction centers were suspended in 10 mM Tris-HCl (pH 8.0), 0.025% lauryl dimethylamine-*N*-oxide and kept frozen at −70°C until used. Bacterial strains from which reaction centers were isolated are named according to the mutation(s) made. The positions of the modified amino acids are indicated in parentheses; they belong to subunit L or M. The modification made is written before the parenthesis (first: wild type; second: mutant). The midpoint redox potentials of the P^+/P couple have been measured in all of the strains (Lin et al., 1994a) and are given in Table 1.

Cytochrome c_2 was prepared as described by Lin et al. (1994b). Measurements were performed with suspensions of reaction centers at ~1 μM in the same medium as above, with the addition of 30 μM cyt c_2, 50 μM 1,4-naphtoquinone, 1 mM sodium ascorbate, and glycerol to a final concentration of 60% v/v.

Measurements of electron transfer kinetics

Kinetics of electron transfer from cyt c_2 to P^+ were measured by flash absorption spectroscopy, essentially as described by Ortega and Mathis (1993) and Venturoli et al. (1993). Reaction centers were excited by a ruby laser flash (~20 ns, 694 nm). The laser flash was of nearly saturating intensity; oversaturation was avoided by decreasing the laser energy with a piece of ground glass and neutral density filters. Formation and decay of P^+ were monitored at 1283 nm, using a laser diode as the source of measuring light and a 0.5-mm diameter germanium photodiode as the detector. Absorption transients were recorded with a transient digitizer with

TABLE 1 P^+/P midpoint potentials and relative amplitudes of the fast exponential components of P^+ decay at $T \geq 270$ K

Strain	*Em*(P^+/P) (mV)*	Amplitude (%)#			$K_{b1} \cdot 10^{-4}$ (M^{-1})§
		Phase 1	Phase 2	Phase 3	
HF(L168)	410	28.0 ± 3.5	16.5 ± 8.3		1.7 ± 0.4
HF(L168) + LH(M160)	485	43.4 ± 2.0	9.2 ± 2.0		3.1 ± 0.3
LH(L131) + HF(L168)	485	21.9 ± 1.5	10.5 ± 1.6		1.1 ± 0.1
Wild type	505	40.3 ± 2.4	6.5 ± 1.0		2.6 ± 0.3
HF(L168) + FH(M197)	545	22.1 ± 2.3	15.6 ± 3.7		1.2 ± 0.2
LH(M160)	565	44.1 ± 6.4	10.5 ± 1.1		3.3 ± 1.0
LH(L131)	585	50.9 ± 2.1	13.6 ± 2.2		4.9 ± 0.6
LH(L131) + LH(M160)	635	33.4 ± 0.5	6.2 ± 1.4	5.9 ± 1.8	2.1 ± 0.1
LH(M160) + FH(M197)	700	20.6 ± 3.5	5.4 ± 2.6	11.8 ± 11.7	1.1 ± 0.3
LH(L131) + FH(M197)	710	21.5 ± 2.0	8.1 ± 2.4	8.1 ± 2.3	1.2 ± 0.2
LH(L131) + LH(M160) + FH(M197)	765	24.1 ± 3.3	8.4 ± 1.7	6.8 ± 1.0	1.3 ± 0.3

*Data from Lin et al. (1994a).

#The relative amplitudes of exponential components obtained from deconvolution of P^+ decay are temperature-independent between 270 K and 295 K within the experimental error. For each phase the values given in the table (as a percentage of the total P^+ signal) are the average and standard deviation over all independent measurements performed at 270 K $\leq T \leq$ 295 K. The relative amplitude of the slow phase is the complement of the amplitudes of the fast components.

§K_{b1}, the apparent binding equilibrium constant for the rapidly reacting complex, is calculated according to Eq. 6.

an electrical bandwidth from DC to 20 MHz. A few measurements of cyt c_2 oxidation in the α-band were made as in Drepper and Mathis (1997).

Reaction centers were placed in a plastic cuvette (optical paths: 1 cm for measuring light, 0.4 cm for excitation) inserted in a holder kept at a controlled temperature. A thermostatted water-ethylene glycol mixture was used in the range 300–240 K; a cryostat cooled with liquid nitrogen was used below 240 K. Unless otherwise specified, kinetic traces are the results of single flash measurements without averaging.

Analysis of data

Deconvolution of P^+ rereduction kinetics into a sum of exponential decays (from three to four components; see Results) was performed by a modified Marquardt algorithm (Bevington, 1969). The success of nonlinear least-squares minimization was judged on the basis of the reduced χ^2 value, χ^2_{min}, and of the distribution of residuals. Care was taken to avoid local minima, by systematically testing the independence of the values finally obtained for the decay parameters from the choice of initial estimates. Over the whole set of absorption transients analyzed, deconvolution yielded well-resolved exponential components with rate constants always differing by at least one order of magnitude. However, given the cross-correlation between deconvolution parameters, confidence intervals were estimated according to the following numerical procedure (Beechem, 1992). For each kinetic trace, to evaluate the error associated with the ith fitting parameter, a series of nonlinear analyses were performed, systematically altering the ith parameter over a range of values. All other fitting parameters were allowed to adjust so as to minimize χ^2 at each value of the ith parameter. An error analysis graph was obtained by plotting the minimized χ^2 versus the value of each fixed ith parameter. The confidence interval was obtained by using an F-statistic to determine the probability p of a particular fractional increase in χ^2 according to

$$\chi^2/\chi^2_{min} = 1 + [m/(n-m)] \cdot F(m, n-m, 1-p) \quad (5)$$

where m is the number of parameters, n is the number of data points, and F is the upper $(1-p)$ quantile for Fisher's F distribution with m and $(n-m)$ degrees of freedom. Confidence intervals within one standard deviation ($p = 0.68$) calculated by this procedure are shown in Fig. 3 for the rate constant of the fast phase of P^+ decay. As a consequence of the nonlinear nature of deconvolution, asymmetrical confidence intervals are generally obtained.

The effect of temperature and free energy on the rate constants obtained from the deconvolution described above was modeled according to conventional electron transfer theory (Eq. 3) and to the more general Eq. 4. Different approaches were tested (see Results), considering the possibility that H bond mutations affect the value of the reorganization energy and/or of the electronic matrix elements. This implied fitting separately subsets of data as well as global data analysis. In all cases, consistency of nonlinear least-squares minimization was checked by using different algorithms (grid search and a modified Marquardt procedure; Bevington, 1969). Global data analysis in terms of Eq. 4 was performed with *Mathematica* programs, using the function *FindMinimum*. In minimizing χ^2, we weighted the values of the rate constant according to the correspondent confidence intervals within one standard deviation determined numerically from the error analysis of P^+ deconvolution. The average of the asymmetrical confidence intervals was used as the weighting experimental uncertainty. Confidence intervals for the parameters of the electron transfer models tested (reorganization energy, electronic coupling term, vibrational frequency) were evaluated by essentially the same procedure as the one applied to deconvolution of absorption transients.

RESULTS

Description of kinetics

Flash excitation of reaction centers leads to an immediate increase of absorption at 1283 nm, followed by a complex decay. These signals are attributed to the very fast oxidation of the primary donor P by light-induced electron transfer and to the subsequent reduction of P^+ by various competing mechanisms. The kinetics in wild-type reaction centers at room temperature have been presented previously, e.g., by Venturoli et al. (1993). The kinetics obtained with two mutants at two temperatures are shown in Fig. 1 as examples, together with a fit into exponential components. The fastest phase (phase 1) is interpreted as an electron transfer from reduced cyt c_2 to P^+ in preformed cytochrome–reaction center complexes in an optimal conformation. A slower

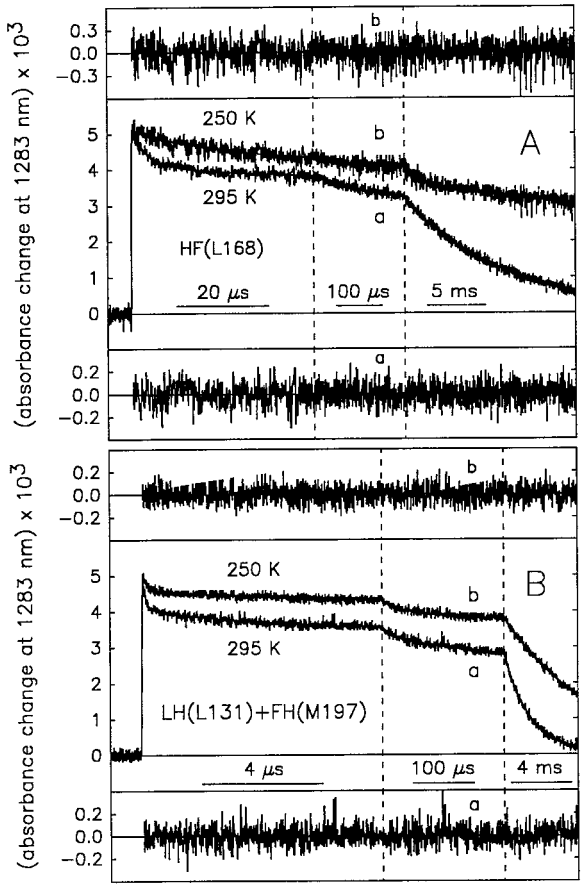

FIGURE 1 Flash-induced absorption changes at 1283 nm induced by a laser flash in RC of the HF(L168) mutant (*A*) and of the LH (L131) + FH(M197) mutant (*B*). Cytochrome c_2 (30 μM) and redox mediators added, as described in Materials and Methods. Measurements at 295 K (*traces a*) and 250 K (*traces b*). Cuvettes with 60% glycerol v/v. Three different sampling rates were used to record absorption changes on time scales going from tens of nanoseconds to several milliseconds. In each panel, residuals are shown from deconvolutions of the signal decay in exponential components with the following characteristics. For HF (L168) (*A*), three phases were used with the following relative amplitudes $A(i)$ and half-times: $A(1) = 20.4\%$, $t_{1/2} = 2.5$ μs; $A(2) = 15.6\%$, $t_{1/2} = 80$ μs; $A(\text{slow}) = 64.0\%$, $t_{1/2} = 6.1$ ms at 295 K (*trace a*); $A(1) = 16.8\%$, $t_{1/2} = 14.2$ μs; $A(2) = 11.1\%$, $t_{1/2} = 569$ μs; $A(\text{slow}) = 72.1\%$, $t_{1/2} = 54$ ms at 250 K (*trace b*). For LH (L131) + FH(M197) (*B*), four phases were necessary for a good fit: $A(1) = 25.4\%$, $t_{1/2} = 71$ ns; $A(2) = 8.6\%$, $t_{1/2} = 2.3$ μs; $A(3) = 7.8\%$, $t_{1/2} = 25$ μs; $A(\text{slow}) = 58.2\%$, $t_{1/2} = 1.2$ ms at 295 K (*trace a*); $A(1) = 12.8\%$, $t_{1/2} = 109$ns; $A(2) = 5.5\%$, $t_{1/2} = 4.8$ μs; $A(3) = 6.8\%$, $t_{1/2} = 35$ μs; $A(\text{slow}) = 74.9\%$, $t_{1/2} = 4.1$ ms at 250 K (*trace b*).

phase (phase 2) is attributed to preformed complexes in a nonoptimal conformation (see Introduction). The slow phase probably results from a diffusion-controlled bimolecular reaction between nonbound cyt c_2 and reaction centers, which is slowed down by viscosity in the presence of glycerol. In the four mutants with the highest P^+/P midpoint potentials, including LH (L131) + FH (M197) in Fig. 1 *B*, a good fit requires a minor additional phase termed phase 3 (see also Table 1). Its half-time was in the range 20–100 μs, and its relative amplitude between 5.9% and 11.8%. It is of unknown origin and it was not studied further in this work.

Phase 1, phase 2, and the slow phase slow down as the temperature is decreased from 295 K (Fig. 1, *curves a*) to 250 K (*curves b*), the effect being more pronounced in the mutant HF(L168) ($Em(P^+/P) = 410$ mV) than in LH (L131) + FH (M197) ($Em(P^+/P) = 710$ mV).

The relative amplitude of the intermediate phase (phase 2) is only 6.5% in wild-type RC, but its extent is up to 16% in some mutants (Table 1). Fig. 2 *A* shows its rate versus free energy for three temperatures (295, 272, and 250 K). The data are rather imprecise, but it is clear that the effect of free energy is qualitatively similar to that on phase 1 (reported in Lin et al., 1994b): a strong acceleration when $-\Delta G°$ increases, an effect that tends to saturate when $-\Delta G°$ is large. The effect of temperature is more important when the free energy is small, in qualitative agreement with the Marcus equation. The rate constant of the slow phase is plotted in Fig. 2 *B* versus free energy, for the same three temperatures. A clear effect of $-\Delta G°$ is observable at 250 K, an effect that is less pronounced at 272 K, and still less at 295 K.

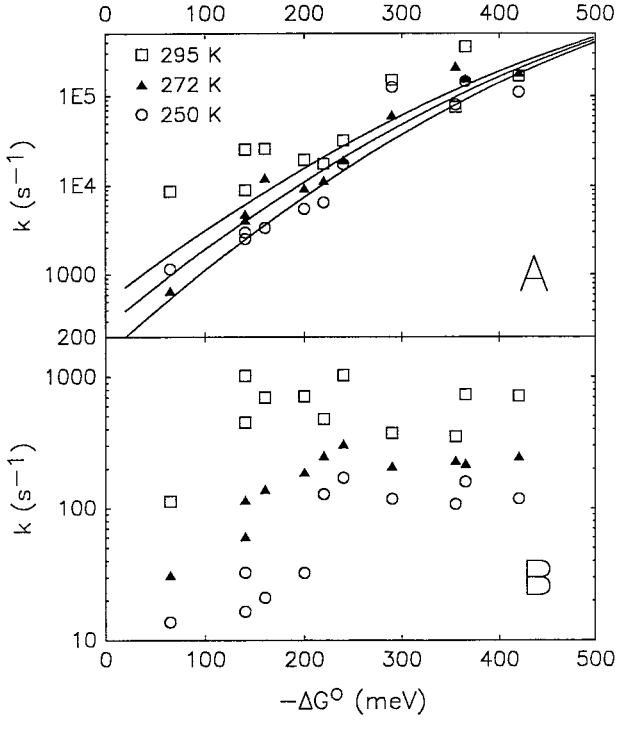

FIGURE 2 Rate of phase 2 (*A*) and of the slow phase (*B*) in the mutants, plotted against $-\Delta G° = Em(P^+/P) - Em(\text{cyt } c_2^{3+}/\text{cyt } c_2^{2+})$, for three temperatures: 295 K (□), 272 K (▲), and 250 K (○). When several kinetic traces were acquired at the same temperature in a given mutant, the average of k values obtained by deconvoluting each independent signal has been plotted. Continuous curves in the upper panel correspond to the global best fit to Eq. 3 at the indicated temperatures (see text for details).

The weight of various phases at $T \geq 270$ K for the studied mutants is given in Table 1. With the hypothesis that phases 1, 2, and 3 are due to preformed RC–cytochrome c_2 complexes, the corresponding apparent binding constants K_{bi} can be calculated according to

$$K_{bi} = (A_i/P) \Big/ \left[\left((C/P) - \sum_{i=1}^{3} A_i \right) \left(1 - \sum_{i=1}^{3} A_i \right) \right] \quad (6)$$

where A_i is the fraction of decay due to the ith phase, P is the total RC concentration, and C is the total cyt c_2 concentration. As shown in Table 1, K_{b1}, the apparent binding constant obtained for the rapidly reacting complex, varies by less than a factor of 5 through the whole set of mutants. The values obtained for K_{b2} (not shown) are two to four times smaller than K_{b1}, depending on the mutant. The binding constant for the rapidly reacting complex has been determined in the same mutants by Lin et al. (1994b) from the amplitude of the fastest phase of P^+ reduction measured over a wide range of cytochrome c_2 concentrations in the absence of glycerol. A correlation plot for K_{b1} in the presence and in the absence of glycerol, based on our estimates and on the data of Lin et al. (1994b), indicates that glycerol affects the binding constant by a similar extent in most of the mutants, decreasing it by a factor of 8 on average (not shown). This decreased affinity when glycerol is added had already been noticed in wild-type reaction centers (Venturoli et al., 1993).

Effect of temperature on the fast phase kinetics

The rate of the fastest phase (phase 1) has been measured for all of the mutants in the temperature range from 295 to 250 K. The data are shown in Fig. 3. The mutants are grouped in two panels for clarity. At room temperature the rates are similar to those published by Lin et al. (1994b) in experiments without glycerol, except that the $t_{1/2}$ are shorter in the present study by a factor of ~1.6. The general trend is that the rate becomes slower when temperature decreases, but the effect is rather small. The Arrhenius plots lead to activation energies between ~5 and 20 kJ · mol^{-1}, except for the mutant LH(L131) + LH(M160), for which an apparent activation energy close to 1 kJ · mol^{-1} is obtained. The limits of a separate analysis of the temperature dependence in each mutant are discussed below in relation to the $\Delta G°$ dependence of the rate constant.

Effect of temperature on the fast phase amplitude

The fraction of P^+ that decays with the fast kinetics is nearly constant between 295 and 270 K. At lower temper-

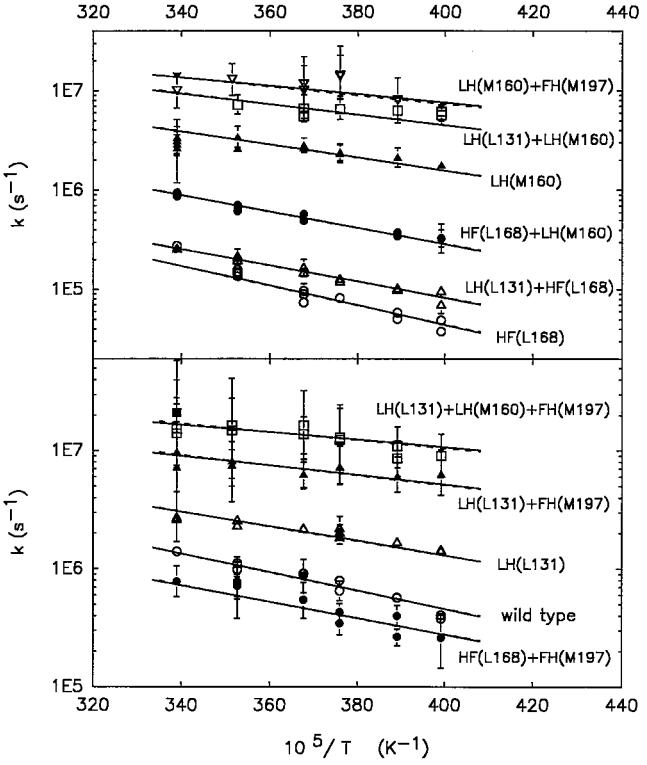

FIGURE 3 Temperature dependence of the rate constant of phase 1 in the mutants. The figure includes the results of direct measurements of cyt c_2 oxidation in the α-band performed in the mutant LH(M160) + FH(M197) (▼) and in the triple mutant LH(L131) + LH(M160) + FH(M197) (■). Vertical bars represent asymmetrical confidence intervals within one standard deviation, calculated as detailed under Materials and Methods. Continuous lines are the result of global analysis according to the Marcus equation (Eq. 3) and correspond to $\lambda = 956$ meV and to the set of electronic terms of Table 2. The dashed lines (almost overlapping with continuous lines) correspond to a global fitting to the Jortner equation (Eq. 4) for $\hbar\omega = 45$ meV, yielding $\lambda = 1205$ meV and the following electronic terms, $H^2_{DA} \times 10^2$ (meV^2): 21.1 (HF(L168)), 28.9 (HF(L168) + LH(M160)), 8.3 (LH(L131) + HF(L168)), 31.0 (wild type), 8.8 (HF(L168) + FH(M197)), 34.2 (LH(M160)), 19.8 (LH(L131)), 29.2 (LH(L131) + LH(M160)), 17.2 (LH(M160) + FH(M197)), 10.2 (LH(L131) + FH(M197)), 9.6 (LH(L131) + LH(M160) + FH(M197)). See text for further details.

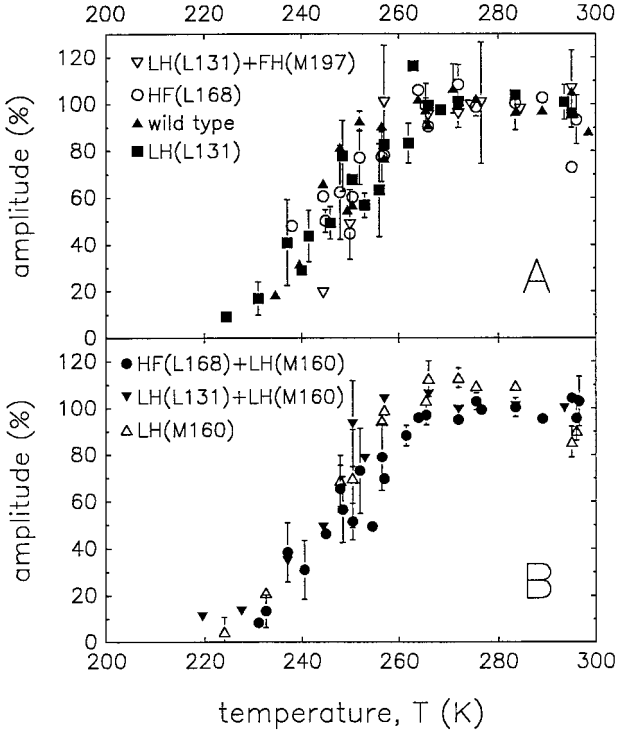

FIGURE 4 Variation with temperature of the relative extent of the fastest phase (phase 1). The percentage amplitude is taken as the value extrapolated at the time of the flash in the deconvolution of the absorption decay into exponential components. To allow a more direct comparison of the temperature dependence, the relative amplitudes in each mutant have been normalized to the maximum extent of the phase observed at room temperature. This plot reports the data obtained with only 7 of the 11 studied mutants, organized in two panels for visual clarity.

atures, the extent of phase 1 decreases to reach nonmeasurable values below 225 K. This phenomenon precludes the study of the phase 1 kinetics below 230 K. The data for seven of the mutants are shown in Fig. 4. They are split into two panels for clarity. All mutants behave nearly identically (the results with four of the mutants are not shown; they are not distinguishable from the others). The temperature at which the fast phase reaches 50% of its maximum value ($T_{1/2}$) is ~246 K.

The relative amplitudes of phases 2 and 3 also decrease when the temperature is lowered below 270–260 K. Their small extent precludes a precise determination of $T_{1/2}$, which, however, is close to that of phase 1. In fact, the contribution of phases 2 and 3 is practically undetectable below 230 K.

Modeling $\Delta G°$ and temperature dependence of the rate constant for intracomplex electron transfer

The free energy dependence of the rate constant k of phase 1 has been examined previously at room temperature in the same set of mutants (Lin et al., 1994b). The data could be fitted to Eq. 3, yielding a reorganization energy $\lambda \approx 500$ meV and a $\Delta G°$-optimized rate constant of 1.4×10^7 s^{-1}. In some of the mutants, however, a pronounced deviation of the experimental k value from the prediction of conventional electron transfer theory was observed. The data acquired in the present study allow a simultaneous analysis of the dependence of the rate upon both temperature and $\Delta G°$, providing a much more severe test of electron transfer theories and constraining the possible choice of parameters more strictly.

The rate constants measured in all of the mutants at all temperatures are plotted in Fig. 5 as a function of $\Delta G° = Em(\text{cyt } c_2^{3+}/\text{cyt } c_2^{2+}) - Em(P^+/P)$. The free energy change for each mutant was evaluated using the data of Table 1 (Lin et al., 1994a) for $Em(P^+/P)$ and assuming $Em(\text{cyt } c_2^{3+}/\text{cyt } c_2^{2+}) = 345$ mV (see Discussion). The data are consistent with two predictions of conventional electron transfer theory: 1) a roughly Gaussian dependence of k upon $-\Delta G°$ at

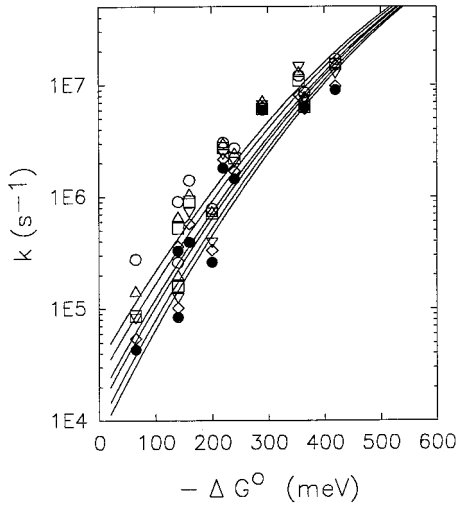

FIGURE 5 $\Delta G°$ dependence of the rate constant of the fast phase (phase 1) at the following six temperatures: 295 K (○), 284 K (△), 272 K (□), 266 K (▽), 257 K (◇), 250 K (●). See the text for the assumptions in evaluating the free energy changes. When several measurements were available at the same temperature in a given mutant, the average value of the rate constants obtained from deconvolution has been plotted (but see Fig. 3, where all single measurements are presented in Arrhenius plots). Continuous curves are best fit to Eq. 3, corresponding to $\lambda = 921$ meV (1σ confidence interval: 812-1036 meV), and $H^2_{DA} = 1.6 \times 10^{-2}$ meV^2 ($(0.50–5.79) \times 10^{-2}$ meV^2), calculated at the six temperatures indicated (*from top to bottom*). At $-\Delta G° = 140$ meV, the upper and lower clusters of data are from mutant HF(L168) + LH(M160) and LH(L131) + HF(L168), respectively.

all temperatures; and 2) a generally less pronounced temperature dependence at increasing values of $-\Delta G°$. Simultaneous best fitting of the measured free energy and temperature dependences to the Marcus equation (Eq. 3) yields a reorganization energy $\lambda = 920 \pm 110$ meV and an electronic coupling $H^2_{DA} = 1.6 \times 10^{-2}$ meV^2. The corresponding predicted free energy dependence is shown in the figure for the six temperature values at which measurements were performed.

Although Eq. 3 gives a reasonable semiquantitative account of both the $\Delta G°$ and the temperature dependence in terms of the same λ and electronic matrix element for all of the mutants, in several mutants experimental k values clearly deviate from the expected behavior. Deviations appear to be systematic (for a given mutant they have a comparable extent at all temperatures), suggesting that at least some of the mutations can specifically affect one or both of the parameters of Eq. 3 (λ and H^2_{DA}) to a different extent. To examine this possibility, we could, in principle, fit the temperature dependence of k to Equation 3 for each mutant individually, thus allowing λ and H^2_{DA} to assume different values in each mutant. Separately fitting the temperature dependencies results in a set of reorganization energies ranging from ~500 meV (in LH(L131) + LH(M160)) to values close to 1200 meV (in HF(L168) + FH(M197) and LH(L131) + LH(M160) + FH(M197)). In the other mutants λ values are grouped between 750 and 1050 meV. The correspondent electronic terms H^2_{DA} cover more than two orders of magnitude (from 7×10^{-4} to 2×10^{-1} meV^2) and appear to be highly correlated with best fitting λ values. A confidence analysis (see Materials and Methods) shows that the uncertainty associated with the parameters is very large, particularly in the electronic terms. Confidence intervals within one standard deviation for H^2_{DA} are highly asymmetrical, and in most of the mutants extend over more than one order of magnitude. The estimated error in the reorganization energy never exceeds 50%, except for the mutant LH(L131) + LH(M160). Although this approach does not yield sound quantitative information, the more limited variation in λ through the set of mutants, as compared to that in H^2_{DA}, leads us to hypothesize that H bond mutations specifically affect the electronic matrix elements to a larger extent. This view is directly supported by a comparison of the temperature dependence in the two double mutants HF(L168) + LH(M160) and LH(L131) + HF(L168). Both mutants have the same $Em(P^+/P) = 485$ mV, i.e., the same driving force for the reaction, but the measured rate constants systematically differ by a factor of 3–4 at all temperatures. The Arrhenius plots in Fig. 3 show that the activation energy E_a is very similar in the two mutants (close to 15 kJ mol^{-1}). Because, according to Eq. 3,

$$E_a = -k_B \partial \ln k / \partial(1/T) = (\lambda + \Delta G^o)^2/4\lambda - k_B T/2 \qquad (7)$$

it can be proposed that the reorganization energy λ is very similar in the two mutants, whereas the electronic coupling has to be different by a factor of 3–4.

On this basis, the optimal choice appears to be a global analysis in which both the $\Delta G°$ and the temperature dependences of k are fitted to Eq. 3, allowing H^2_{DA} to assume a different value in any mutant, but using the same value of λ for all of the mutants. Further arguments supporting this choice are examined in the Discussion. Under this constraint, a satisfactory fit can be obtained (see the *continuous curves* in the Arrhenius plots of Fig. 3), characterized by a reduced χ^2 very close to 1 (1.038). This global analysis yields $\lambda = 956$ meV, with a confidence interval within one standard deviation ranging from 888 meV to 1023 meV. The best fitting values obtained for the electronic coupling terms H^2_{DA} vary by no more than a factor of 4 through the whole set of mutants and are given in Table 2 with the corresponding confidence intervals. In conclusion, the data can be modeled acceptably in the framework of conventional electron transfer theory, i.e., by assuming that the electron transfer is coupled only to low-frequency vibrations such that $\hbar\omega \ll k_B T$ and that nuclear motions can be treated classically. Over our experimental T range, this means vibrational energies lower than 20 meV (160 cm^{-1}).

In more general theories, this limitation has been removed by quantum mechanical treatments of the nuclear coordinates. Equation 4 (Jortner, 1976) is obtained by considering the donor and the acceptor coupled to a single harmonic vibrational mode of frequency ω. At "low" fre-

TABLE 2 Electronic coupling terms obtained by global analysis of data according to the Marcus equation, using the same value of the reorganization energy for all of the mutants studied

Strain	$H_{DA}^2 \times 10^2$ (meV^2)	$k_{opt} \times 10^{-8}$ (s^{-1})	d (Å)
HF(L168)	3.60 (1.60–7.70)	6.2	10.5
HF(L168) + LH(M160)	4.96 (2.40–10.50)	8.6	10.3
LH(L131) + HF(L168)	1.42 (0.60–2.81)	2.5	11.2
Wild type	5.36 (2.50–11.25)	9.3	10.2
HF(L168) + FH(M197)	1.53 (0.72–3.34)	2.6	11.1
LH(M160)	6.00 (2.80–12.3)	10.4	10.2
LH(L131)	3.50 (1.70–7.00)	6.1	10.5
LH(L131) + LH(M160)	5.24 (2.50–11.00)	9.1	10.3
LH(M160) + FH(M197)	3.26 (1.66–6.58)	5.6	10.6
LH(L131) + FH(M197)	1.91 (0.90–4.10)	3.3	11.0
LH(L131) + LH(M160) + FH(M197)	1.87 (0.90–3.80)	3.2	11.0

The heme-P distances d are calculated from the $\Delta G°$-optimized rate constants k_{opt}, according to the model of Moser et al. (1992). See text for further details.

quency ($\hbar\omega \ll k_BT$) this equation reproduces the predictions of Eq. 3. At "intermediate" frequencies ($\hbar\omega \cong 2k_BT$), Eq. 4 is, in principle, still compatible with the moderate positive activation energies observed over the temperature range examined, but gives rise to a free energy and temperature dependence quite distinct from that predicted by conventional electron transfer theory. We therefore tested the possibility that Eq. 4 could describe our full set of data with an accuracy equal to or better than that of Eq. 3. The following global analysis procedure was adopted: the vibrational frequency ω was fixed at a given value, and the weighted global χ^2 was minimized in terms of the reorganization energy λ (assumed to be the same for all of the mutants) and of a set of 11 electronic coupling terms H_{DA}^2, which were allowed to vary from one mutant to another. The effect of the vibrational frequency in fitting to Eq. 4 was explored by iterating this procedure for values of $\hbar\omega$ ranging from 1 meV to 100 meV (i.e., from the classical limit to vibrational energies close to 800 cm^{-1}).

Fig. 6 *A* shows the minimized reduced χ^2 as a function of the vibrational frequency. The corresponding best fitting values obtained for the reorganization energy λ and for the electronic terms are plotted in Fig. 6 *B* and Fig. 6, *C* and *D*, respectively. The best description of the data in terms of Eq. 4 is obtained for "low" frequencies, i.e., $\hbar\omega \leq 10$ meV. Over this range of frequencies, nuclear motion can be treated classically, and fitting to Eq. 4 yields the same parameter values as global analysis in terms of the Marcus equation. When the vibrational frequency is fixed at progressively higher values, the minimized χ^2 increases smoothly. At $\hbar\omega \cong 2k_BT$ (45 meV), the minimized χ^2 is still well below the confidence level within one standard deviation of the minimum χ^2 obtainable by fitting to Eq. 3. At these intermediate frequencies (~350 cm^{-1}), the fit is slightly worse than at "low" frequencies; however, an acceptable account of the free energy and temperature dependences of the rate constant can still be obtained by optimization of λ and of the electronic terms. As an example, the best fit to Eq. 4 with $\hbar\omega = 45$ meV is shown (*dashed lines*) in the Arrhenius plots of Fig. 3; in all of the mutants, the

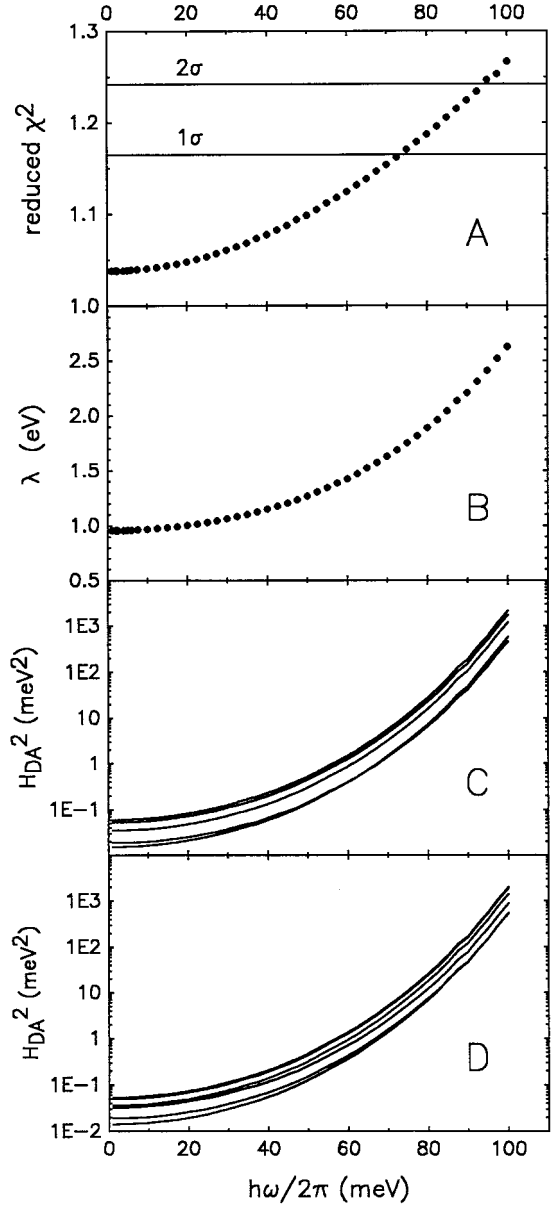

FIGURE 6 Global analysis of data according to the Jortner equation (Eq. 4). Details of the fitting procedure are given in the Results and in Materials and Methods. (*A*) The weighted reduced χ^2 minimized at each value of the vibrational frequency is plotted versus $\hbar\omega$. The horizontal lines give χ^2 confidence levels for a global fit to the Marcus equation (Eq. 3). They were calculated with Eq. 5 (see Materials and Methods), with $\chi^2_{min} = 1.038$ for $p = 0.68$ (1σ) and $p = 0.95$ (2σ). (*B*) Best fitting values of the reorganization energy as a function of the vibrational energy. Each data point is the result of a numerical nonlinear minimization. (*C* and *D*) Corresponding electronic coupling terms H_{DA}^2 versus energy of the vibrational mode coupled to the reaction. The curves (*from top to bottom*) are for the following mutants: LH(M160), LH(L131) + LH(M160), LH(L131), LH(L131) + LH(M160) + FH(M197), HF(L168) + FH(M197) in *C*; wild type, HF(L168) + LH(M160), HF(L168), LH(M160) + FH(M197), LH(L131) + FH(M197), LH(L131) + HF(L168) in *D*.

predicted temperature dependence is hardly distinguishable from that obtained at "low" frequency, i.e., by global fitting to the Marcus equation. Best fitting to Eq. 4 at $\hbar\omega = 45$ meV requires a considerable adjustment in the parameters of electron transfer with respect to the values obtained at "low" frequency: the reorganization energy increases to 1205 meV, and the electronic terms are larger by a factor of ~6 on average (see the legend of Fig. 3). This is a general trend: when higher frequencies are imposed, both the reorganization energy and the electronic terms have to be increased considerably (see Figs. 6 *B*, and 6, *C* and *D*). In summary, the analysis in terms of the Jortner equation indicates that the most accurate description of the data is obtained in the classical limit at $\hbar\omega \leq 10$ meV; however, we cannot exclude with high confidence the possibility that vibrational frequencies corresponding to 40–50 meV are coupled to the reaction.

The temperature and $\Delta G°$ dependences of the rate constant for the intermediate phase (phase 2) of P^+ reduction have been analyzed in the framework of conventional electron transfer theory, following essentially the same criteria as were applied to phase 1. A rough description of the $\Delta G°$ and temperature dependence can be obtained in the hypothesis that the mutations do not greatly perturb the values of the electronic matrix element and the reorganization energy. Under this assumption, best fitting to Eq. 3 yields $\lambda = 823$ meV (1σ confidence interval (730–934 meV)) and $H^2_{AB} = 8.6 \times 10^{-5}$ meV^2 ($(3.3–27.3) \times 10^{-5}$ meV^2). The free energy dependence of these parameters is plotted for three temperatures in Fig. 2 *A*. The experimental errors associated with *k* values appear to be considerably larger for phase 2 (see Fig. 2 *A*), presumably as a consequence of its relative amplitude, which is systematically lower than that of phase 1 (see Table 1). In contrast with what is found for the fastest phase, in the case of phase 2, adjusting the tunneling matrix elements for the individual mutants with the constraint of a single value for the reorganization energy leads to a little improvement of the quality of the fit and to a substantial indetermination in the values of the parameters. Following this approach, the 1σ confidence interval for the reorganization energy ranges from 690 to 1880 meV, and the corresponding intervals for the H^2_{AB} always extend over several orders of magnitudes. The large scattering of data does not allow us to examine possible specific effects of the H bond mutations on the electronic matrix elements for phase 2.

DISCUSSION

Estimation of electron transfer parameters for the fastest intracomplex reaction: assumptions and implications

The series of hydrogen bond mutants used in the present investigation provides a valuable tool for examining the effect of free energy on the rate of intracomplex electron donation from cyt c_2 to P^+. A previous study performed at 295 K in the absence of cryosolvents (Lin et al., 1994b) has shown that the altered midpoint potential of P^+/P is the main parameter affected by the mutations, resulting in a Marcus-type dependence of the first-order rate constant on the exothermicity of the reaction. Fitting the data obtained under these conditions to the Marcus equation (Eq. 3) sets a lower limit of the reorganization energy around 500 meV.

In this work, $\Delta G°$ and temperature dependences have been considered simultaneously, to achieve a more stringent test of Marcus-type relations and a possibly more reliable evaluation of the parameters controlling the reaction rate. At 295 K, in all of the mutants, our rate constants are higher by a factor of ~1.6 compared with those measured by Lin et al. (1994b) in the absence of glycerol. The same accelerating effect of glycerol has been reported for wild-type RCs (Venturoli et al., 1993) and has also been observed more recently in the fast phases of P^+ reduction in a cross-linked RC–cyt c_2 complex (Drepper et al., 1997). It has been proposed by these authors that the effect arises from an increase of the driving force, possibly due to a slight decrease ($\cong$ 30 mV) in the midpoint potential of cyt c_2.

In qualitative agreement with the prediction of Marcus-type models, the effect of temperature is generally more pronounced at low driving force (see Figs. 3 and 5). Given the assumption that neither the reorganization energy λ nor the tunneling matrix element is affected by the mutations, we fitted the data taken at all temperatures to the Marcus equation (Eq. 3), obtaining $\lambda = 920 \pm 110$ meV and $H^2_{DA} \cong 1.6 \times 10^{-2}$ meV^2. Although χ^2 analysis, taking into account the confidence intervals of the deconvoluted rate constants, indicates a quantitatively unacceptable fit, these values provide a rough account of free energy dependence. It is noteworthy that, under such a restrictive hypothesis, Eq. 3 also reproduces the extent to which temperature affects the rate in the different mutants. As shown in Fig. 5, however, the experimental values are offset significantly from the theoretical predictions in most of the mutants. The determined λ and H^2_{DA} are therefore to be regarded as average values; the two parameters could be modulated to different extents in each mutant, causing the observed deviations from the calculated values.

As outlined in the Results, the limited temperature range accessible and the high correlation between H^2_{DA} and λ preclude a meaningful evaluation of the two parameters in each mutant from individual temperature dependencies. We therefore performed a global fitting in which the electronic term could vary among the mutants, while keeping a common reorganization energy for the whole set. This view is supported by several arguments:

1. Two mutants (HF(L168) + LH(M160) and LH(L131) + HF(L168)), characterized by the same $\Delta G°$ ($Em(P^+/P) = 485$ mV), exhibit rate constants systematically differing by a factor of 3–4 over the whole temperature range. Because the activation energy is very similar in these two double mutants ($\cong$ 15 kJ mol^{-1}), the observed difference in rate is ascribable mainly to a different tunneling matrix element.

2. Despite the large uncertainties associated with the determination of λ and H^2_{DA} when the temperature depen-

dence is fitted separately for each mutant, the variation in the electronic terms appears to be much larger than that in λ.

3. The reorganization energy in proteins or protein complexes is often split into additive contributions from redox groups and different protein and solvent domains (Marcus and Sutin, 1985; McLendon and Hake, 1992). Because the special pair P is embedded in a rather rigid and hydrophobic environment, the prevailing contribution to the reorganization energy in the RC–cyt c_2 complex is likely to be due to repolarization of the solvent, of cytochrome c_2 chromophore and protein medium, and perhaps of the interface between the donor and acceptor proteins. These terms are not expected to differ greatly in the different mutants (see below).

4. The hydrogen bond mutations examined in this work are confined to a region close to the special dimer, deep in the protein, and should not interfere greatly with the binding of cyt c_2. In the presence of glycerol, we have obtained similar binding constants K_{b1} ranging from 1.1 to 4.9×10^4 M^{-1} throughout the whole set of mutants (see Table 1). The limited extent of variation of the affinity indicates that the rapidly reacting RC–cyt c_2 complex is not substantially perturbed by the mutations. Nevertheless, the observed variability in K_{b1} is likely to reflect a series of slightly different conformations of the complex, which could mainly affect the electronic term through changes in distance, relative orientation of the chromophores, or relative contributions of different tunneling paths.

5. Alterations in the optical spectra of the RC for some of the mutants (particularly LH(L131) + HF(L168) and HF(L168) + FH(M197)) (Lin et al., 1994a) suggest small changes in the three-dimensional electronic structure of the special bacteriochlorophyll pair. Studies based on Fourier transform Raman (Mattioli et al., 1994) and ENDOR spectroscopy (Rautter et al., 1995) indicate that the addition or removal of a hydrogen bond causes large shifts in the spin density in the cation radical P^+ between the two halves (P_L and P_M) of the dimer. Rautter et al. (1995) have shown that over the set of mutants studied, the fraction of the spin density on the L-half (ρ_L) ranges from 0.22 in LH(L131) + HF(L168) to 0.83 in LH(M160) + FH(M197). Using the data at 295 K of Lin et al. (1994b), these authors have proposed that the electronic coupling H^2_{DA} changes in correlation with ρ_L (Rautter et al., 1995, 1996).

If H^2_{DA} is allowed to vary among the mutants, while keeping the assumption that reorganization energy is not affected by the mutations, the Marcus equation (Eq. 3) adequately fits the dependence of the rate constant k on both $\Delta G°$ and temperature (see Fig. 3, *continuous lines*). This global analysis, despite the large number of fitting parameters (11 electronic matrix elements plus λ), yields a well-defined χ^2 minimum ($\chi^2_\nu = 1.038$), with $\lambda = 956 \pm 68$ meV and a set of H^2_{DA} differing by no more than a factor of 4 (see Table 2). The correlation between λ and H^2_{DA} in Eq. 3 is mainly reflected in fairly large and asymmetrical confidence intervals for the electronic terms.

In performing the analysis described above, we evaluated the free energy change from the midpoint redox potentials of the reactants, assuming that $\Delta G° \approx Em(\text{cyt } c_2^{3+}/\text{cyt } c_2^{2+}) - Em(P^+/P)$. This approximation does not take into account that solvation energies of the redox centers in the free proteins may differ from those in the complex and that electrostatic interactions between cofactors may be different in the reactant and product state. However, these contributions tend to balance each other, so that the error in the calculated $\Delta G°$ is expected to be small (see Alden et al., 1995, and references therein). We used the data of Lin et al. (1994a) for $Em(P^+/P)$ (see Table 1) and a midpoint potential for cyt c_2, $Em(\text{cyt } c_2^{3+}/\text{cyt } c_2^{2+}) = 345$ mV, based on measurements performed in chromatophores from *Rb. sphaeroides* (Meinhardt and Crofts, 1982) and in solution (Pettigrew et al., 1975; Prince and Bashford, 1979). The same value was used in the study at 295 K by Lin et al. (1994b). A recent determination for free cyt c_2 from *Rb. sphaeroides* in solution gives a value of 335 mV at pH 8.0 (Drepper et al., 1997). Cross-linking of cyt c_2 to the RC affects the redox properties of the heme, leading to disappearance of the pH dependence of the midpoint potential and to an *Em* value of 370 mV between pH 7.5 and 9.5 (Drepper et al., 1997). Using this *Em* would decrease our ($-\Delta G°$) values by 25 meV. On the other hand, the presence of glycerol might compensate for this effect by decreasing the redox potential of cyt c_2 by ~30 mV (see above and Drepper et al., 1997).

Electrostatic effects associated with the charge separated state $P^+Q_A^-$ could also systematically affect the actual value of the driving force in all of the mutants. In *Rps. viridis* the reduced primary acceptor Q_A^- formed upon flash excitation has been calculated to perturb the redox equilibrium between P and cyt *c*-559 by 55 mV (Gao et al., 1990). Although estimates of electrostatic interactions based on the notion of an effective dielectric constant in proteins are problematic (see e.g., Harvey, 1989), in view of the strong structural and functional similarities between the two systems, a comparable electrostatic perturbation within the cyt c_2–RC complex of *Rb. sphaeroides* can be hypothesized, leading to a corresponding decrease in the ($-\Delta G°$) values. This effect, added to a possible shift of 25 mV in the *Em* of cyt c_2 in the complex, would decrease the driving force by 80 meV.

The systematic uncertainty in the $\Delta G°$ values marginally affects the information drawn from the global fitting to Eq. 3. A uniform decrease by 80 meV in ($-\Delta G°$) with respect to the values assumed in the analysis described above would shift the reorganization energy from 956 meV down to 815 meV. Over this extent of $\Delta G°$ variation, the maximum relative changes in H^2_{DA} range from ~5% to 25%, being progressively more pronounced in mutants with higher P^+/P midpoint potentials. Interestingly, the quality of the fit is slightly improved when ($-\Delta G°$) values are uniformly decreased ($\chi^2_\nu = 0.994$ for a decrease of 80 meV).

A growing body of evidence suggests that the reorganization energies associated with interprotein electron transfer involving cytochrome *c* may be rather large. Recently Muegge et al. (1997) have calculated the reorganization energy of equine cytochrome *c*, using the reduced and

oxidized NMR solution structures of the protein. They found a value of λ between ~400 and 700 meV, which is larger than that previously evaluated using crystal structures of the protein (Churg et al., 1983), but still considerably lower than estimates based on analysis of the self-exchange reaction (Marcus and Sutin, 1985). By interpreting driving-force effects on rates in terms of the Marcus equation, reorganization energies have been suggested for electron transfer between cytochrome *c* and cyt *c* peroxidase (~1.4 eV) (McLendon and Hake, 1992), in ruthenated cytochrome *c* derivatives (~1.2 eV) (Meade et al., 1989), and for the monomolecular electron transfer within the cyt *c*–cyt b_5 complex (~0.7–0.8 eV) (McLendon and Miller, 1985; McLendon, 1988). The reorganization energy obtained by us for electron transfer within the RC–cyt c_2 complex falls in the 0.7–1.4 eV range, which encompasses previous estimates for electron transfer in noncovalent protein complexes formed by cytochrome *c*.

In the simplest view, the value of the tunneling matrix element H_{DA} is considered to be determined mainly by the edge-to-edge distance between donor and acceptor through an exponential dependence (Eq. 2). Moser et al. (1992) have shown that, for several electron transfer reactions in purple bacterial reaction centers, free-energy optimized rates can be roughly described by such a relation, assuming an electron transfer rate of 10^{13} s^{-1} at van der Waals contact (d_o = 3.6 Å) and an exponential coefficient of decay $\beta = 1.4$ $Å^{-1}$. A first difficulty in quantitatively assessing rate-distance relationships arises from the necessity of properly factoring out the Franck-Condon nuclear contribution; uncertainties in the reorganization energy (often encompassing a few hundreds of meV) can considerably distort the determination of the optimized rate. The H_{DA}^2 values determined by our global fit yield $\Delta G°$ optimized rate constants ranging from 2.5×10^8 s^{-1} (in LH(L131) + HF(L168)) to 10.4×10^8 s^{-1} (in LH(M160)). The corresponding edge-to-edge distances (*d*) calculated according to the relationship of Moser et al. (1992) are summarized in Table 2. In wild-type RC, a distance $d = 10.2$ Å is obtained.

The precise binding site of cyt c_2 on the RC and the orientation of cyt c_2 within the complex that optimizes electron donation are a matter of investigation. Different structures have been proposed, all involving electrostatic interactions between lysine residues surrounding the heme crevice of the cytochrome and negatively charged carboxylate groups on the periplasmic surface of the RC. In the model of Allen et al. (1987), using the three-dimensional structure of *Rhodospirillum rubrum* cyt c_2, the cytochrome was placed nearly symmetrically over the primary donor in a position analogous to that of the *Rps. viridis* cytochrome, and then rotated to maximize the number of charge pair interactions, resulting in a distance of closest approach between the heme ring and the special pair of 11 Å. This docking, which keeps the heme coplanar with the bacteriochlorophyll rings, is rendered unlikely by linear dichroism data (Tiede, 1987; Drepper and Mathis, 1997) and by site-directed mutagenesis studies probing the periplasmic RC binding surface (Adir et al., 1996; Tetreault et al., 1997). In a second model (Tiede et al., 1988; Tiede and Chang, 1988), based on electrostatic energy minimization and accommodating optical dichroism data, the cytochrome is shifted toward the M side of the RC surface and displaced further from the RC (the heme iron-to-bacteriochlorophyll magnesium distance is 23 Å, as compared to a separation of 19 Å in the model proposed by Allen et al., 1987). Recently x-ray diffraction data from a cocrystal of the RC and cyt c_2 have been used to obtain the three-dimensional structure of the complex (Adir et al., 1996). In the derived model, cyt c_2 is shifted toward the M side of the RC even more than in the Tiede model, yielding an edge-to-edge distance between the heme and the special pair P of the RC of ~14 Å.

The structural models available for the complex indicate a range of edge-to-edge distances (11–14 Å) not incompatible but clearly larger than the values of 10–11 Å calculated from our data on the basis of the empirical relationship of Moser et al. (1992). Several reasons may account for this apparent discrepancy. First of all, as pointed out by Tiede and Chang (1988), the separation between the cytochrome and the RC in docking models should be taken as an upper limit, because mutual amino acid side-chain rearrangements can lead to closer association of the redox partners. The limits of the approach of Moser et al. (1992), as well as those of more sophisticated treatments considering specific electron tunneling pathways, have been thoroughly debated, emphasizing possible ambiguities in the identification of a proper boundary between the donor and acceptor molecules and the groups of the intervening medium (Farid et al., 1993; Friesner, 1994). Using the pathway model of Beratan and Onuchic, Aquino et al. (1995) examined the electronic matrix element for two docked cyt c_2 structures, one based on the Tiede and Chang model (Tiede and Chang, 1988), and the other based on maximizing electronic coupling, obtaining very similar electronic coupling decays. However, their pathway analysis resulted in an underestimated electron transfer rate when they used the prefactor ($\approx 10^{13}$ s^{-1}) that appears to apply to ruthenated cytochromes. Again, these authors underline the possible relevance of dynamic fluctuations of the proteins in reducing distances and thereby enhancing through-space electronic coupling.

The variation in H_{DA}^2 values through the series of mutants may reflect a change in distance between heme and P, in their mutual orientation, in the selection or relative weight of different tunneling pathways, or in the electronic structure of the special bacteriochlorophyll pair, as well as combinations of these factors. When ascribed mainly to a different distance between the chromophores, the model of Moser et al. (1992) would predict a maximum change of ~1 Å.

For some of the mutants, a pronounced deviation of the experimental rate constants from the Marcus equation was already observed when the $\Delta G°$ dependence was fitted in the absence of glycerol at 295 K (Lin et al., 1994b). Rautter et al. (1995, 1996) have proposed that these deviations, attributed to alterations of the electronic term, correlate with

the asymmetrical distribution of the π-spin density between the L- and M-halves of P^+. Our temperature dependence analysis indicates that the deviations observed at 295 K systematically occur over the 250–300 K temperature range and are plausibly accounted for by a different electronic factor H_{DA}^2 in each mutant. Fig. 7 shows that the H_{DA}^2 values obtained, although subject to a large experimental uncertainty, exhibit some correlation ($R \cong 0.6$) with the fraction of the spin density on the L-half of P^+ determined by ENDOR investigations. As discussed by Rautter et al. (1996), if the electron transfer proceeds through the HOMO of P^+, this would indicate a more favorable coupling between the heme and the L-half of the dimer.

The Marcus equation (Eq. 3) assumes a classical view of nuclear motions, i.e., that the electron transfer is coupled only to vibrations of frequency ω such that $\hbar\omega \ll k_B T$. Over the temperature range of our measurements, this implies vibrational energies lower than 20 meV (160 cm^{-1}). The possible involvement of higher frequency modes has been examined by performing a global analysis according to Eq. 4, which is the simplest equation incorporating quantum mechanical effects for a single vibrational mode. A single reorganization energy, common to all of the mutants, and a set of 11 electronic coupling terms H_{DA}^2 were used as parameters of the fit. The ability of the Jortner equation to describe the observed temperature and $-\Delta G°$ dependence was tested for vibrational energies ranging from the classical limit to 100 meV ($\sim$800 cm^{-1}). The minimum reduced χ^2 (χ_ν^2) is obtained at very low frequencies, when the predictions of Marcus and Jortner equations coincide. The quality of the fit, however, depends rather smoothly upon the value of the coupled vibrational frequency, so that "intermediate" frequencies (e.g., $\sim$350 cm^{-1}) at $\hbar\omega \cong 2k_B T$ are still quite compatible with the data (cf. Fig. 3, *dashed lines*, and Fig. 6 *A*). At these frequencies, although the calculated values of the rate constants are very close to the Marcus prediction over the $\Delta G°$ and temperature range of the experimental data, both the estimated reorganization energy (Fig. 6 *B*) and the tunneling matrix elements (Fig. 6, *C* and *D*) are systematically and markedly increased. These adjustments yield progressively higher $\Delta G°$-optimized rate constants. In the model of Moser et al. (1992), correspondingly shorter edge-to-edge distances are obtained, which become progressively incompatible with current structural data. At $\hbar\omega = 45$ meV, e.g., an optimized rate constant $k_{opt} \cong 5 \times 10^9$ s^{-1} can be calculated by using Eq. 4 for wild-type RC (as compared to $k_{opt} \cong 9 \times 10^8$ s^{-1} in the Marcus limit), which in turn places the redox cofactors at a distance $d \cong 9$ Å. In summary, analysis in terms of the Jortner equation indicates that a classical treatment of nuclear motions is more appropriate and sets an upper limit to the average frequency of coupled vibrations close to 20–30 meV.

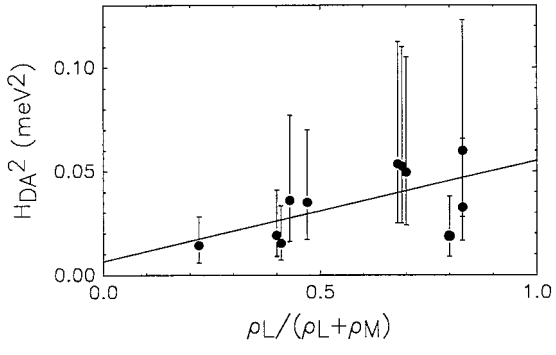

FIGURE 7 Correlation plot between the electronic coupling terms H_{DA}^2 derived from global fitting to the Marcus equation and the fraction of spin density ρ on the L-half of the special pair P. The values of $\rho_L/(\rho_L + \rho_M)$ are taken from Rautter et al. (1996).

Behavior at low temperature

The study of the temperature dependence of the rate constant for the fast intracomplex electron donation is precluded below 250 K because, in all of the mutants examined, the relative amplitude of phase 1 falls off drastically at low temperatures (Fig. 4). This behavior has been documented in wild-type RCs, both in detergent and when reconstituted into liposomes (Venturoli et al., 1993). In *Rps. viridis* reaction centers, under redox conditions in which only the highest potential heme (*c*-559) of the bound tetraheme subunit is reduced, a similarly abrupt inhibition of electron transfer to P^+ occurs within the same narrow temperature range (Ortega and Mathis, 1993). A similar effect is seen in a covalently stabilized cross-linked complex between cyt c_2 and the RC of *Rb. sphaeroides* (Drepper et al., 1997). These observations suggest that the disappearence of the fast phase of electron donation reflects an inhibition of the intracomplex electron transfer process, rather than dissociation of the complex (Venturoli et al., 1993).

It seems unlikely that a structural change of the complex, affecting the electronic coupling through an increase in the heme–P^+ distance, is responsible for the inability of cyt *c* to reduce P^+ at low temperatures. According to Moser et al. (1992), a decrease in the rate by a factor of 10^3-10^4 would require an increase in the edge-to-edge distance by 5–7 Å. A sudden disruption of the dominant electron tunneling pathways is also unlikely to occur over the same temperature range in structurally different systems.

In *Rps. viridis* RC, the transition temperature $T_{1/2}$, at which the fast phase amplitude of P^+ reduction is decreased to 50% of its maximum, is shifted from $\sim$250 K when only the high-potential heme is reduced to 210 K and 80 K, respectively, when two hemes (*c*-559 and *c*-556) and three hemes (*c*-559, *c*-556, *c*-552) are reduced before photoexcitation (Ortega and Mathis, 1993). A temperature-induced perturbation of the electronic term would not easily account for this dependence upon the redox state of the tetraheme. As proposed by Ortega and Mathis (1993), we therefore consider it likely that in both systems (*Rps. viridis* and *Rb. sphaeroides*) the energetics of the electron transfer process

undergo a drastic change at low temperature, affecting the relative values of $-\Delta G°$ and λ.

Our present results show that the temperature range over which the intracomplex electron transfer is inhibited is the same in all of the mutants ($T_{1/2} \cong 250$ K), i.e., independent of the reaction exothermicity, at least for 65 meV $< -\Delta G°$ $<$ 420 meV at high temperature. This indicates that blocking of the reaction cannot be due simply to a continuous temperature dependence of the driving force, resulting from different temperature dependencies of the *Em* values of the two redox centers.

A reasonable possibility is that, over the narrow temperature range of the transition, medium reorganization that substantially compensates for the charge displacement coupled to electron transfer is blocked by freezing. Structural rearrangements associated with cyt c_2 oxidation and involving the protein medium as well as bound water molecules would be hindered at low temperature. This could result in a substantial destabilization of the product of electron transfer, i.e., in a sudden increase in the effective $\Delta G°$ not compensated by a decrease in λ. The possible freezing out of different structural reorganizations accompanying cyt *c* oxidation both in the cyt c_2–RC complex from *Rb. sphaeroides* and in the *Rps. viridis* reaction centers has been discussed extensively (see Mathis et al., 1994; Ortega et al., 1997), placing a special emphasis on the role of structured water molecules.

The insensitivity of the transition temperature $T_{1/2}$ to the altered *Em* of the P^+/P couple in the hydrogen bond mutants examined suggests that the destabilization of the oxidized form of cyt c_2 at low temperature is too large to be overcome by a 350-mV increase in the redox potential of the special pair. If this is correct, the variation in $T_{1/2}$ in *Rps. viridis* RC according to the redox state of the hemes is likely to reflect mainly a local electrostatic perturbation of the medium surrounding cyt *c*-559 induced by prereduction of hemes *c*-556 and *c*-552, rather than a decrease in its *Em*. This change in the *Em* has been estimated to be only 14 mV and 77 mV, respectively, upon reduction of *c*-556 and *c*-552 (Gunner and Honig, 1991).

$\Delta G°$ and temperature effects on the kinetics of the slower phases of P^+ rereduction

The intermediate phase of P^+ reduction (phase 2) is ~50 times slower than phase 1. Its rate constant is strongly affected by the *Em* of the P^+/P couple and exhibits a temperature dependence similar to that of phase 1 in all the mutants. Fitting to the Marcus equation (Eq. 3) provides a reasonable account of the $\Delta G°$ and temperature dependence of the rate constant, yielding an estimate of the reorganization energy ($\lambda = 820 \pm 100$ meV) comparable to the value determined for phase 1. The corresponding electronic term, H_{DA}^2, is more than two orders of magnitude smaller than the average value for the fastest intracomplex reaction. The large experimental error precludes an analysis of possible effects of mutations on the tunneling matrix element.

These results indicate that the slower rate of phase 2 is not due to energetic factors, and suggest that phase 2 reflects electron donation from cyt c_2 docked in a nonoptimal conformation. The Marcus fit to the $\Delta G°$ and temperature dependence of the rate of phase 2 corresponds at $-\Delta G° = \lambda$ to a maximum rate constant $k_{opt} = 1.6 \times 10^6\ s^{-1}$, as compared to $k_{opt} = 2.8 \times 10^8\ s^{-1}$ calculated from the fit to the rate constant of phase 1, assuming the same λ and electronic coupling in all of the mutants. Using the empirical distance dependence of Moser et al. (1992), these values would translate into a distance between the heme and the primary donor that is longer by ~3.7 Å in the nonoptimal conformation. Recent studies of a cross-linked complex between cyt c_2 and the RC (Drepper et al., 1997; Drepper and Mathis, 1997) revealed the existence of two conformations, giving rise to electron transfer to P^+ characterized by similar activation energies and by half-lives comparable to those of phase 1 and phase 2 in the present work.

On the basis of previous studies in wild-type RC (Venturoli et al., 1993; Tiede et al., 1993; Wang et al., 1994), the slow phase of P^+ reduction can be ascribed mainly to a second-order collisional reaction between the RC and free reduced cyt c_2. Under our measuring conditions, the half-life of the slow phase lies between ~1 ms and 70 ms. Over this time range, charge recombination of the flash-induced $P^+Q_A^-$ state is expected to compete with the oxidation of cyt c_2 in reducing the primary donor. The observed rate constant of the slow phase of P^+ reduction, k_{obs}, will therefore be the sum of the rate constant of the back-reaction (k_{br}) and the rate constant (k_s) of electron donation by free cytochrome: $k_{obs} = k_{br} + k_s$. In seven of the mutants used in the present investigation, k_{br} has been measured under the same experimental conditions as in our study over a wide temperature range (Ortega et al., 1996), allowing an estimate of k_s values. The contribution of k_{br} to k_{obs} is negligible at high temperatures, but increases to 20–50% at 250 K, because of slowing down of cyt c_2 oxidation.

The corrected pseudo-first-order rate constants k_s have been converted into true second-order rate constants, k, by dividing by the concentration of free cytochrome c_2. The resulting $\Delta G°$ dependence is shown in Fig. 8 at three temperatures. In wild-type RC at room temperature, a value of k around $2 \times 10^7\ M^{-1}\ s^{-1}$ is obtained, similar to that determined previously in the presence of glycerol (Venturoli et al., 1993). As already apparent from the uncorrected values of k_{obs}, the effect of $\Delta G°$ on the rate of the bimolecular reaction is quite different from the effects on the faster phases (phase 1 and 2) ascribed to intracomplex electron donation. The rate constant increases with $-\Delta G°$ up to ~150–250 meV; at higher $-\Delta G°$, the rate constants level off to free energy-independent values. This trend is also observed at the other intermediate temperatures investigated (cf. Fig. 2 *B*, in which data at 272 K and for all the mutants are included). The saturation in the $-\Delta G°$ dependence appears to shift to slightly higher exothermicities at low temperature. The leveling of the rate constant suggests that

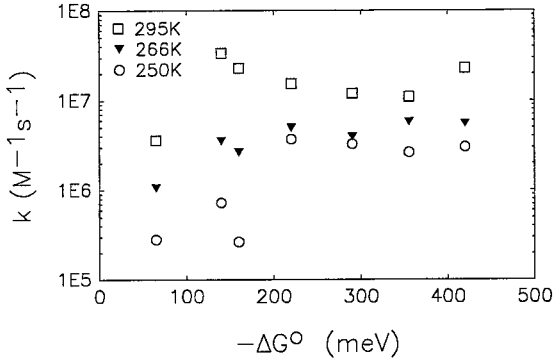

FIGURE 8 Free energy dependence of the second order rate constant k calculated from the pseudo-first-order rate of the slow P^+ decay corrected for contributions due to charge recombination of the $P^+Q_A^-$ state. See text for further details.

the collisional reaction is partially diffusion controlled, reaching the diffusion limit at high driving force (Marcus and Sutin, 1985). The strong temperature dependence of the viscosity of a 60% v/v glycerol-water mixture between 295 K and 250 K (see Newman, 1968) may be responsible for the large effect of temperature (about one order of magnitude) on the asymptotic rate constant.

This work was supported by the National Science Foundation (MCB-9404925), by the Consiglio Nazionale delle Ricerche, and by the Ministero della Università e della Ricerca Scientifica e Tecnologica of Italy. FD acknowledges the financial support provided by the European Community (HCM programme).

REFERENCES

Adir, N., H. L. Axelrod, P. Beroza, R. A. Isaacson, S. H. Rongey, M. Y. Okamura, and G. Feher. 1996. Co-crystallization and characterization of the photosynthetic reaction center-cytochrome c_2 complex from *Rhodobacter sphaeroides*. *Biochemistry.* 35:2535–2547.

Alden, R. G., W. W. Parson, Z. T. Chu, and A. Warshel. 1995. Macroscopic and microscopic estimates of the energetics of charge separation in bacterial reaction centers. *In* The Reaction Center of Photosynthetic Bacteria. Structure and Dynamics. M.-E. Michel-Beyerle, editor. Springer-Verlag, Berlin. 105–116.

Allen, J. P., G. Feher, T. O. Yeates, H. Komiya, and D. C. Rees. 1987. Structure of the reaction center from *Rhodobacter sphaeroides* R-26: the protein subunits. *Proc. Natl. Acad. Sci. USA.* 84:6162–6166.

Aquino, A. J. A., P. Beroza, D. N. Beratan, and J. N. Onuchic. 1995. Docking and electron transfer between cytochrome c_2 and the photosynthetic reaction center. *Chemi. Phys.* 197:277–288.

Beechem, J. M. 1992. Global analysis of biochemical and biophysical data. *Methods Enzymol.* 210:37–54.

Beratan, D. N., J. N. Betts, and J. N. Onuchic. 1991. Protein electron transfer rates set by the bridging secondary and tertiary structure. *Science.* 252:1285–1288.

Bertrand, P. 1991. Application of electron transfer theories to biological systems. *Structure Bond.* 75:1–47.

Bevington, P. R. 1969. Data Reduction and Error Analysis for the Physical Sciences. McGraw-Hill, New York.

Boxer, S. G. 1990. Mechanisms of long-distance electron transfer in proteins: lessons from photosynthetic reaction centers. *Annu. Rev. Biophys. Biophys. Chem.* 19:267–299.

Churg, A. K., R. M. Weiss, A. Warshel, and T. Takano. 1983. On the action of cytochrome *c*: correlating geometry changes upon oxidation with activation energies of electron transfer. *J. Phys. Chem.* 87: 1683–1694.

DeVault, D. 1984. Quantum-Mechanical Tunnelling in Biological Systems. Cambridge University Press, Cambridge.

Drepper, F., P. Dorlet, and P. Mathis. 1997. Cross-linked electron transfer complex between cytochrome c_2 and the photosynthetic reaction center of *Rhodobacter sphaeroides*. *Biochemistry.* 36:1418–1427.

Drepper, F., and P. Mathis. 1997. Structure and function of cytochrome c_2 in electron transfer complexes with the photosynthetic reaction center of *Rhodobacter sphaeroides*: optical linear dichroism and EPR. *Biochemistry.* 36:1428–1440.

Farid, R. S., C. C. Moser, and P. L. Dutton. 1993. Electron transfer in proteins. *Curr. Opin. Struct. Biol.* 3:225–233.

Feher, G., T. R. Arno, and M. Y. Okamura. 1988. The effect of an electric field on the charge recombination rate of $D^+Q_A^-\rightarrow DQ_A$ in reaction centers from *Rhodobacter sphaeroides* R-26. *In* The Photosynthetic Bacterial Reaction Center. J. Breton and A. Vermeglio, editors. Plenum, New York. 271–287.

Friesner, R. A. 1994. Comparison of theory and experiment for electron transfers in proteins: where's the beef? *Structure.* 2:239–343.

Gao, J., R. J. Shopes, and C. A. Wraight. 1990. Charge recombination between the oxidized high-potential *c*-type cytochromes and Q_A^- in reaction centers from *Rhodopseudomonas viridis. Biochim. Biophys. Acta.* 1015:96–108.

Gunner, M. R., and P. L. Dutton. 1989. Temperature and $-\Delta G°$ dependence of the electron transfer from BPh^- to Q_A in reaction center protein from *Rhodobacter sphaeroides* with different quinones as Q_A. *J. Am. Chem. Soc.* 111:3400–3412.

Gunner, M. R., and B. Honig. 1991. Electrostatic control of midpoint potentials in the cytochrome subunit of the *Rhodopseudomonas viridis* reaction center. *Proc. Natl. Acad. Sci. USA.* 88:9151–9155.

Harvey, S. C. 1989. Treatment of electrostatic effects in macromolecular modeling. *Proteins.* 5:78–92.

Hopfield, J. 1974. Electron transfer between biological molecules by thermally activated tunneling. *Proc. Natl. Acad. Sci. USA.* 71: 3640–3644.

Jortner, J. 1976. Temperature dependent activation energy for electron transfer between biological molecules. *J. Chem. Phys.* 64:4860–4867.

Karpishin, T. B., M. W. Grinstaff, S. Komar-Panicucci, G. McLendon, and H. B. Gray. 1994. Electron transfer in cytochrome *c* depends upon the structure of the intervening medium. *Structure.* 2:415–422.

Kuki, A., and P. G. Wolynes. 1987. Electron tunneling paths in proteins. *Science.* 236:1647–1652.

Lin, X., H. A. Murchison, V. Nagarajan, W. W. Parson, J. P. Allen, and J. C. Williams. 1994a. Specific alteration of the oxidation potential of the electron donor in reaction centers from *Rhodobacter sphaeroides. Proc. Natl. Acad. Sci. USA.* 91:10265–10269.

Lin, X., J. C. Williams, J. P. Allen, and P. Mathis. 1994b. Relationship between rate and free energy difference for electron transfer from cytochrome c_2 to the reaction center in *Rhodobacter sphaeroides. Biochemistry.* 33:13517–13523.

Long, J. E., B. Durham, M. Okamura, and F. Millett. 1989. Role of specific lysine residues in binding cytochrome c_2 to the *Rhodobacter sphaeroides* reaction center in optimal orientation for rapid electron transfer. *Biochemistry.* 28:6970–6974.

Marcus, R. A., and N. Sutin. 1985. Electron transfers in chemistry and biology. *Biochim. Biophys. Acta.* 811:265–322.

Mathis, P., J. M. Ortega, and G. Venturoli. 1994. Interaction between cytochrome *c* and the photosynthetic reaction center of purple bacteria: behaviour at low temperature. *Biochimie.* 76:569–579.

Mattioli, T. A., J. C. Williams, J. P. Allen, and B. Robert. 1994. Changes in primary donor hydrogen-bonding interactions in mutant reaction centers from *Rhodobacter sphaeroides*: identification of vibrational frequencies of all the conjugated carbonyl groups. *Biochemistry.* 33: 1636–1643.

McLendon, G. 1988. Long-distance electron transfer in proteins and model systems. *Acc. Chem. Res.* 21:160–167.

McLendon, G., and R. Hake. 1992. Interprotein electron transfer. *Chem. Rev.* 92:481–490.

McLendon, G., and J. R. Miller. 1985. The dependence of biological electron transfer rates on exothermicity: the cytochrome *c*/cytochrome b_5 couple. *J. Am. Chem. Soc.* 107:7811–7816.

Meade, T. J., H. B. Gray, and J. R. Winkler. 1989. Driving-force effects on the rate of long-range electron transfer in ruthenium-modified cytochrome *c*. *J. Am. Chem. Soc.* 111:4353–4356.

Meinhardt, S. W., and A. R. Crofts. 1982. Kinetic and thermodynamic resolution of cytochrome c_1 and cytochrome c_2 from *Rhodopseudomonas sphaeroides*. *FEBS Lett.* 149:223–227.

Moser, C. C., J. M. Keske, K. Warmcke, R. S. Farid, and P. L. Dutton. 1992. Nature of biological electron transfer. *Nature.* 355:796–802.

Muegge, I., P. X. Qi, A. J. Wand, Z. T. Chu, and A. Warshel. 1997. The reorganization energy of cytochrome *c* revisited. *J. Phys. Chem. B.* 101:825–836.

Newman, A. A. 1968. Glycerol. Morgan-Grampian, London.

Ortega, J. M., B. Dohse, D. Oesterhelt, and P. Mathis. 1997. Very fast electron transfer from cytochrome to the bacterial photosynthetic reaction center at low temperature. *FEBS Lett.* 401:153–157.

Ortega, J. M., and P. Mathis. 1993. Electron transfer from the tetraheme cytochrome to the special pair in isolated reaction centers of *Rhodopseudomonas viridis*. *Biochemistry.* 32:1141–1151.

Ortega, J. M., P. Mathis, J. C. Williams, and J. P. Allen. 1996. Temperature dependence of the reorganization energy for charge recombination in the reaction center from *Rhodobacter sphaeroides*. *Biochemistry.* 35: 3354–3361.

Overfield, R. E., C. A. Wraight, and D. DeVault. 1979. Microsecond photooxidation kinetics of cytochrome c_2 from *Rhodopseudomonas sphaeroides*: in vivo and solution studies. *FEBS Lett.* 105:137–142.

Pan, L., J. T. Hazzard, J. Lin, G. Tollin, and S. I. Chan. 1991. The electron input to cytochrome *c* oxidase from cytochrome *c*. *J. Am. Chem. Soc.* 113:5908–5910.

Parson, W. W., and A. Warshel. 1995. Theoretical analyses of electron transfer reactions. *In* Anoxygenic Photosynthetic Bacteria. R. E. Blankenship, M. T. Madigan, and C. E. Bauer, editors. Kluwer Academic Publishers, Dordrecht, the Netherlands. 559–575.

Pettigrew, G. W., T. E. Meyer, R. G. Bartsch, and M. D. Kamen. 1975. pH dependence of the oxidation-reduction potential of cytochrome c_2. *Biochim. Biophys. Acta.* 430:197–208.

Prince, R. C., and C. L. Bashford. 1979. Equilibrium and kinetic measurements of the redox potentials of cytochromes c_2 in vitro and in vivo. *Biochim. Biophys. Acta.* 547:447–454.

Rautter, J., F. Lendzian, X. Lin, J. C. Williams, J. P. Allen, and W. Lubitz. 1996. Effect of orbital asymmetry in $P^{\cdot+}$ on electron transfer in reaction centers of *Rb. sphaeroides*. *In* The Reaction Center of Photosynthetic Bacteria. Structure and Dynamics. M.-E. Michel-Beyerle, editor. Springer-Verlag, Berlin. 37–50.

Rautter, J., F. Lendzian, C. Shulz, A. Fetsch, M. Kuhn, X. Lin, J. C. Williams, J. P. Allen, and W. Lubitz. 1995. ENDOR studies of the primary donor cation radical in mutant reaction centers of *Rhodobacter sphaeroides* with altered hydrogen-bond interactions. *Biochemistry.* 34: 8130–8143.

Tetreault, M., S. H. Rongey, G. Feher, and M. Y. Okamura. 1997. Mapping the cyt c_2 binding site of the RC:cyt c_2 complex using site-directed mutagenesis. *Biophys. J.* 72:A7.

Tiede, D. M. 1987. Cytochrome *c* orientation in electron-transfer complexes with photosynthetic reaction centers of *Rhodobacter sphaeroides* and when bound to the surface of negatively charged membranes: characterization by optical linear dichroism. *Biochemistry.* 26:397–410.

Tiede, D. M., D. E. Budil, J. Tang, O. El-Kabbani, J. R. Norris, C. H. Chang, and M. Schiffer. 1988. Symmetry breaking structures involved in the docking of cytochrome *c* and primary electron transfer in reaction centers of *Rhodobacter sphaeroides*. *In* The Photosynthetic Bacterial Reaction Center: Structure and Dynamics. NATO ASI Sries A: Life Sciences, Vol. 149. J. Breton and A. Vermeglio, editors. Plenum Press, New York. 13–20.

Tiede, D. M., and C. H. Chang. 1988. The cytochrome *c* binding surface of reaction centers from *Rhodobacter sphaeroides*. *Isr. J. Chem.* 28: 183–191.

Tiede, D. M., and P. L. Dutton. 1993. Electron transfer between bacterial reaction centers and mobile *c*-type cytochromes. *In* The Photosynthetic Reaction Center. J. Deisenhofer and J. R. Norris, editors. Academic Press, New York. 257–288.

Tiede, D. M., A. C. Vashishta, and M. R. Gunner. 1993. Electron transfer kinetics and electrostatic properties of the *Rhodobacter sphaeroides* reaction center and soluble *c*-cytochromes. *Biochemistry.* 32: 4515–4531.

Venturoli, G., A. Mallardi, and P. Mathis. 1993. Electron transfer from cytochrome c_2 to the primary donor of *Rhodobacter sphaeroides* reaction center. A temperature dependence study. *Biochemistry.* 32: 13245–13253.

Wang, S., X. Li, J. C. Williams, J. P. Allen, and P. Mathis. 1994. Interaction between cytochrome c_2 and reaction centers from purple bacteria. *Biochemistry.* 33:8306–8312.